EVALUATING NEUTRON EFFECTIVE DOSE BY MONTE CARLO SIMULATION

YUNJIN AHN, GI-SUB KIM, TAEHWAN KIM AND SANGROK KIM*
** Radiation Safety Section, Korea Institute of Radiological and Medical Sciences, Seoul, Korea*
**E-mail: kim@kirams.re.kr*

Abstract: Recently, a new radiation treatment method using a high-energy accelerator facility has attracted attention. High-energy particles used in radiation therapy react with structures in the treatment room and generate secondary radiation, X-rays, and neutrons. In particular, neutrons have a higher biological weight than photons and are more harmful to normal tissue. However, CR-39, a general-purpose neutron dosimeter, cannot measure high-dose and high-energy neutrons. Therefore, this study calculated the neutron effective dose inside the high-energy accelerator irradiation room using the WWS and WWR functions of MCNP 6.2 to confirm the effective neutron dose that can be generated inside the high-energy accelerator room. And this result can be used to evaluate the neutron effective dose when an accident occurs inside the high-energy accelerator irradiation room.

Keywords: *Secondary radiation, MCNP, Particle therapy, Radiation therapy*

1. INTRODUCTION

A high-energy accelerator is a device that accelerates particles such as electrons and protons and is used in various fields such as medical, research, and industry [1-2]. In the medical field, high-energy accelerators are used for cancer treatment. Cancer treatment using X-rays and electron beams accelerated using high-energy accelerators is a universal radiation treatment method worldwide [3]. Such radiation treatment requires minimizing damage to normal tissues during the treatment process [4]. Recently, proton and heavy ion therapy have gained attention because they offer better treatment outcomes and cause fewer side effects than traditional radiation therapy using X-ray or electron beams [5]. However, this therapy is known to produce more secondary radiation than traditional radiation therapy.

Secondary radiation generated in radiation therapy reaches the patient and the operators; and causes additional exposure [3,6]. This exposure occurs in particle therapy using high energy and radiation therapy using low energy, which is undesirable [6-7]. According to International Commission on Radiological Protection (ICRP) report 103, such exposure is classified as medical exposure. And ICRP recommends that medical exposure to patient is controlled with a reference level. The CR-39, a personal dosimeter commonly used for evaluating effective neutron dose, cannot measure high-dose up to 60 mSv. Therefore, calculations are required to handle this exposure.

Monte Carlo N-Particle (MCNP) developed by the Los Alamos National Laboratory in the United States, a particle transport simulation, is a universal code for accurate radiation dose calculation. This code is useful for calculating radiation doses, which are difficult to measure radiation directly [8-9]. When this code is used for shielding calculations for radiation protection, it takes a long time to calculate due to radiation attenuation. In this process, various functions provided by MCNP are useful to reduce the calculation time.

In a radiation exposure accident, the dose in the irradiation room is crucial to calculate the dosage received quickly. However, CR-39, a commonly used personal dosimeter, cannot be utilized in facilities with high doses. Therefore, this study aims to evaluate the neutron effective dose by the MCNP 6.2 and evaluate inside the high-energy accelerator irradiation room for the radiation exposure accident.

2. THE MAIN PART OF REPORT

2. 1. Research subjects and methodology

Neutrons were measured at the Korea Institute of Radiological and Medical Sciences (KIRAMS) high-Energy accelerator irradiation room. This irradiation room has been used for neutron therapy since 1986 but is currently operated as a beam irradiation facility for research. Protons accelerated by the MC50 cyclotron irradiate a beryllium target to generate neutrons. The energies used for proton acceleration are 30 and 40 MeV. The beam port provided by KIRAMS is divided into vertical and horizontal beams. In this experiment, the vertical beam irradiation port of Fig. 1 was applied. Neutrons are generated at vertical beam ports on the gantry. Also, the thickness of the beryllium target inside the gantry is 1.05 cm. If the beryllium target is not thick enough, a proton beam accelerated to high energy can pass through the beryllium target.

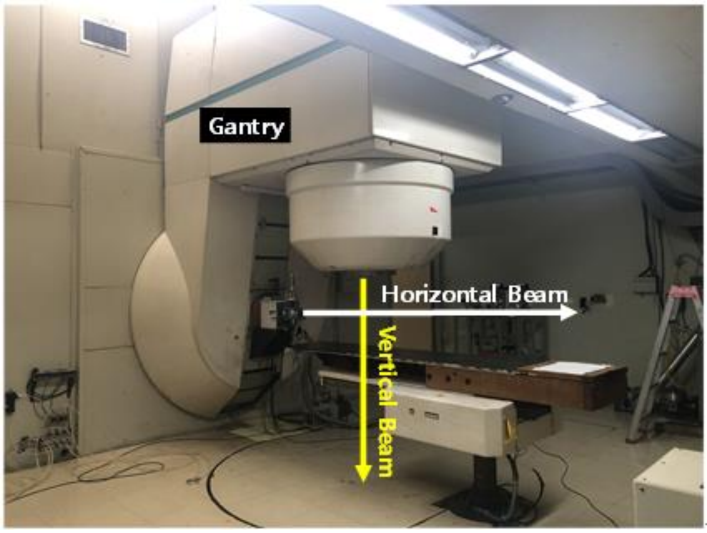

Fig. 1. High-energy accelerator irradiation room in Korea Institute of Radiological and Medical Sciences used in this study. The gantry have been fixed. The vertical and horizontal beam are serving to researchers.

In this study, the neutron dose was calculated using MCNP 6.2. The geometry for simulation should be implemented similarly to the actual experimental environment. However, some structures were omitted depending on the type of radiation being measured. In this study, the geometry consisted of a concrete wall, a beryllium target, an aluminum filter, a detector, and a gantry. The schematic diagram of the implemented high-energy accelerator irradiation room is shown in Fig. 2. The detector is 120 cm away from the floor of the irradiation chamber, and the beryllium target and detector are located about 5 m apart. The cross-section of the implemented gantry structure is detailed in Fig. 3.

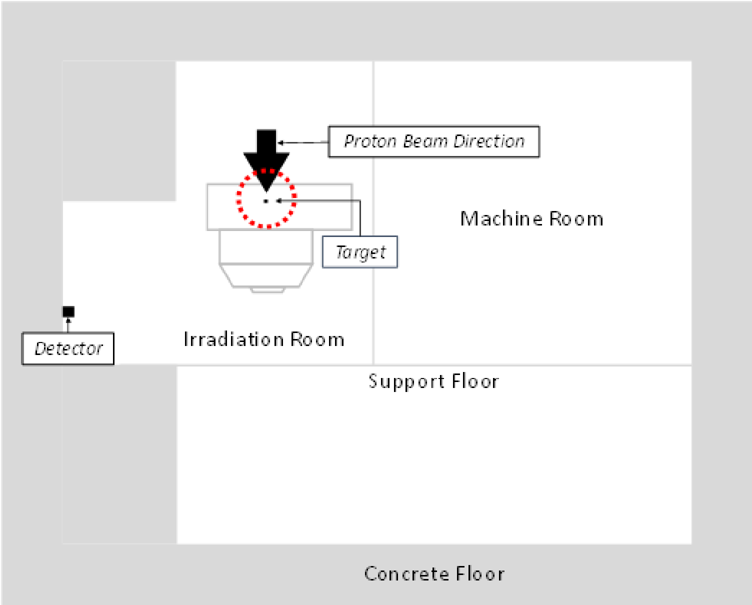

Fig. 2. Cross-sectional view of the irradiation room. The detector for used in the calculation is away 120 cm from the irradiation room floor.

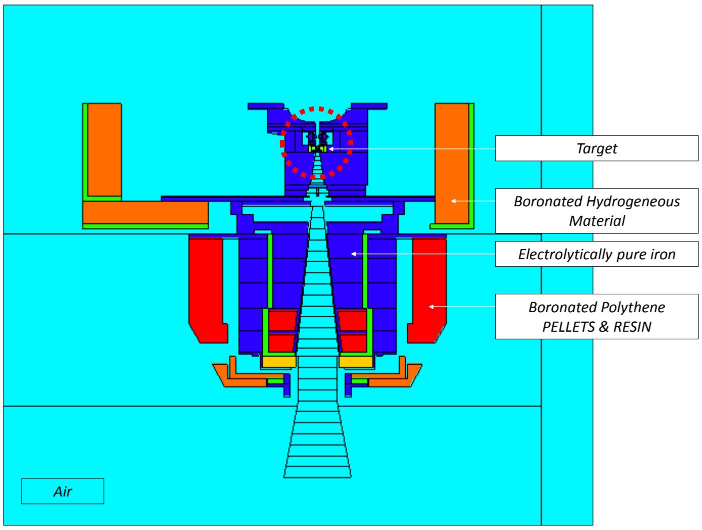

Fig. 3. Cross-sectional view of gantry implemented by simulation and major materials

The material designation is essential for the implemented geometry to obtain nuclear reaction results. Some compositions of materials were taken from the previous study [10] and the other materials are assumed with chemical composition and density [11].

Protons colliding with the Be target for neutron generation were designated as the radiation source. The selected radiation source was a pen beam-type proton with 20, 30, or 40 MeV energy. Protons irradiated at a location 0.5 cm away from the beryllium target started in the -1 cm direction in the Z axis of a vertical experiment and the -1 cm direction in the X axis in the case of a horizontal investigation. In the particle transport process, protons and neutrons are calculated.

In the simulation with nuclear reactions, computational functions are very important as they reduce the time to reach reliable results. However, when using on the Windows operating system, only one thread is available for proton computation by MCNP 6.2. Therefore, Surface Source Write (SSW) and Surface Source Read (SSR) functions were used to reduce calculation time for neutrons. The SSW function is used to collect neutron data generated within a specified range near the radiation source. The data collection section was designated as a sphere centered on the source. The diameter of the sphere is 180 cm, and all gantry structures are included. Outside of this sphere, data collection is unnecessary, so important is set to zero. SSW data collection was conducted for 1,200 minutes. The collected neutron data were used for calculation using the SSR function. For the SSR run, the radiation source is removed, and the particle of interest is excluded protons. The surface to which the SSR function will be applied has been specified, and the important in the area that needs to be calculated has been changed to one. And the neutron data imported into the SSR can modify the coordinates. Proton particles are not used in the calculation process using the SSR function. Therefore, the multi-thread function could be used. The number of threads used is 30.

In this study, the neutron effective dose was calculated using MCNP 6.2. The neutron dose conversion factor for Anterior-Posterior direction provided in ICRP Report 116 was applied during the calculation process [12].

2. 2. Results

The neutron particle distribution collected using the SSW function is shown in Fig. 4. The calculated history for 1,200 minutes is 550,882,440 at 30 MeV and 189,324,716 at 40 MeV. The radiation source and beryllium target were located inside the red zone. Most of the neutrons are shielded by the gantry, and the neutrons pass through the collimator and appear as an isocentric beam. The irradiation field of this neutron beam is 26 by 26 cm.

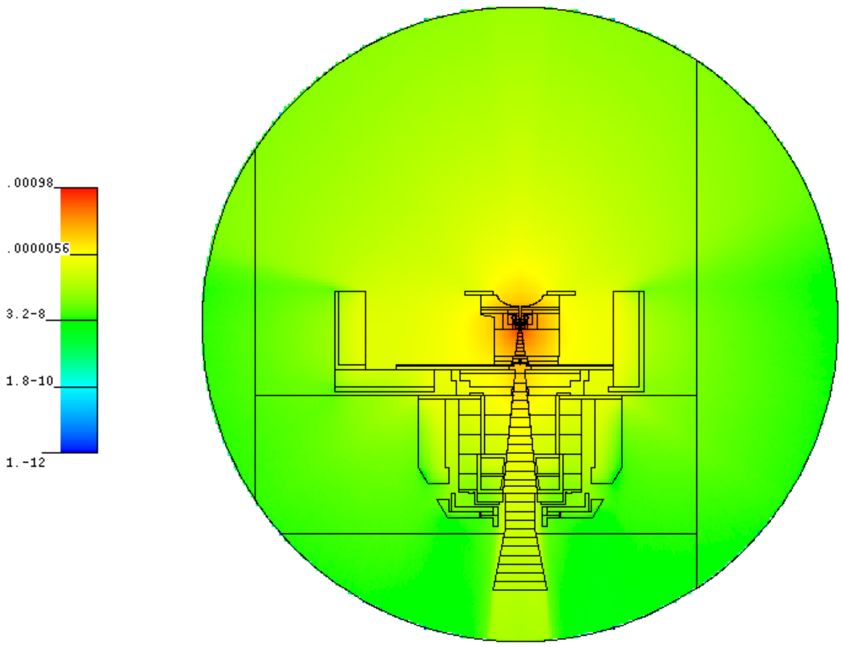

Fig. 4. In the SSW calculation using proton irradiation, the neutron dose map is the cross-sectional view of the gantry with 40 MeV proton condition.

The neutron dose distribution and error image calculated by the SSR function are shown in Fig. 5, and the area where the detector location is additionally displayed on the image. The error of the detector zone was 0.12 under the 30 MeV condition and 0.16 under the 40 MeV condition. The simulation calculation number has reached the maximum. The calculated histories is 9,843,208 under the 30 MeV condition and 8,598,727 under the 40 MeV condition.

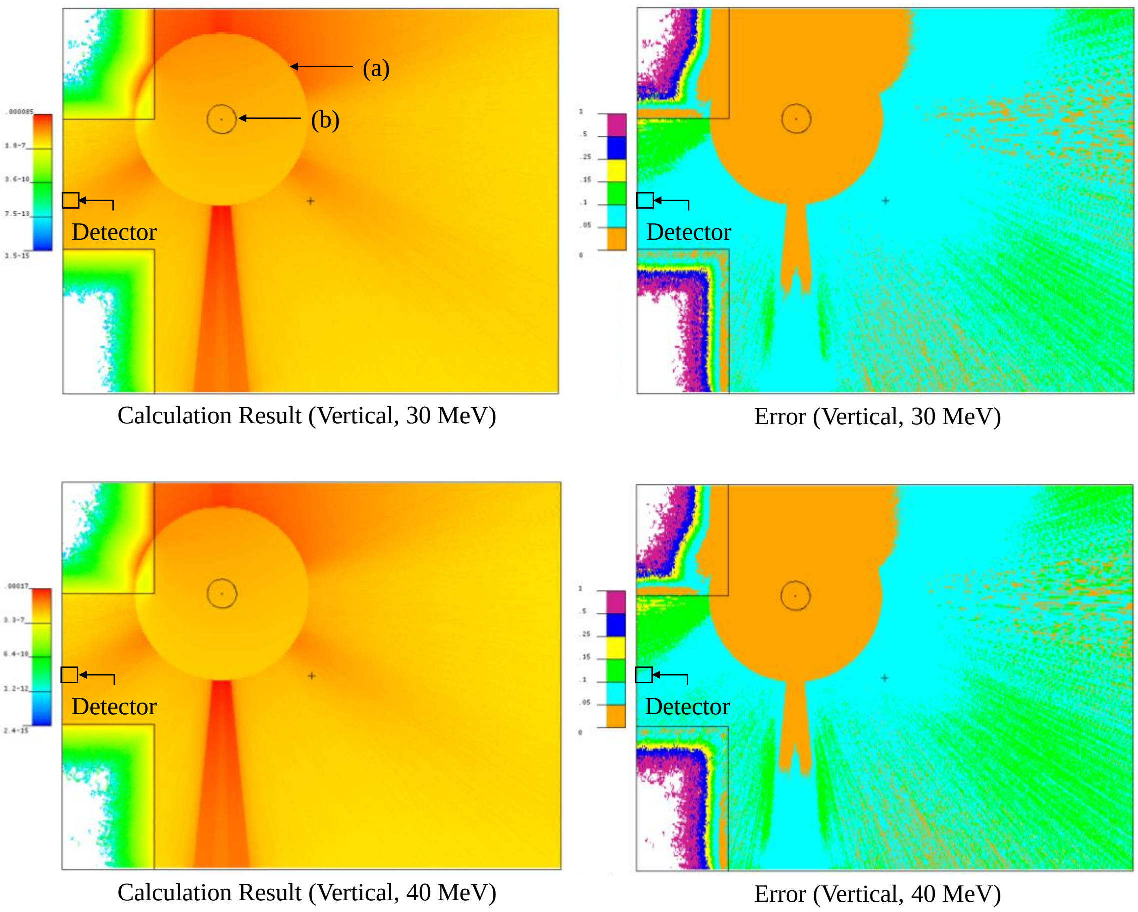

Fig. 5. Calculated neutron effective dose map and relative error using the SSR function of MCNP 6.2. The (a) is the sphere border that outside was calculated using the neutron particle data collected by the MCNP 6.2's SSW function. The (b) is the location of the beryllium target.

The calculation results of MCNP 6.2 are shown in Table 1. When a 30 MeV proton beam has a charge of 300 μA·sec, the neutron effective dose is 2.49 mSv. When a 40 MeV proton beam has a charge of 300 μA·sec, the effective dose of neutrons is 5.76 mSv. These two results can be expressed in Eq. (1). y is the calculated neutron effective dose by MCNP 6.2, a is a constant, and x is the charge amount. Under the same charge condition, the neutron dose is higher when the proton acceleration energy is 40 MeV than 30 MeV.

$$\boldsymbol{y = ax} \tag{1}$$

Table 1. The result of neutron dose calculation by MCNP 6.2

Beam direction	**Proton energy**	**Electric charge (μA·sec)**	**Neutron effective dose (mSv)**	***a***
Vertical	30 MeV	300	2.49	0.0083
	40 MeV	300	5.76	0.0192

2. 3. Discussion

The distribution of neutrons generated inside the radiation treatment room was calculated using MCNP 6.2. The boron is a gantry constituent material and is advantageous for thermal neutron shielding. Therefore, MCNP calculation results showed that most of the neutrons were shielded by being surrounded by the gantry. As a result, there was expected to be a difference in the neutron dose distribution depending on the existence of the gantry structure.

In MCNP 6.2, fluence is defined as the number of particles per unit area. Fluence is high in the area close to the radiation source and rapidly decreases when it is shielded. In Fig. 4, the neutrons in the unshielded area show about 175 times higher fluence. At this time, an area with low fluence will require a longer time if an accurate result value is to be derived. And in Fig. 5, the neutrons were shielded by the concrete wall, and the uncalculated area appeared white. Even if these areas were calculated over a long time, the calculated dose would not be reliable. This result should be taken into account when designing the simulation.

In the calculated results, when the proton energy increased from 30 MeV to 40 MeV, the effective neutron dose in the detector area increased 2.3 times. Therefore, the neutron dose should also be evaluated in the therapy room using accelerated carbons up to 430 MeV [10-11].

3. CONCLUSION

This study calculated the neutron effective dose generated inside the radiation therapy room using MCNP 6.2. In the calculation result in the high-energy accelerator irradiation facility, the calculation time was shortened using the SSW and SSR functions. However, the relative errors of calculation results in some region were greater than 0.1. This phenomenon is considered a limitation of the maximum number of histories in the SSR function.

This calculated dose and distribution can be used to evaluate exposure amount when a radiation exposure accident occurs inside the irradiation room. In future works, the effective neutron dose inside the irradiation room using a dosimeter will be measured to compare these experimental measurements with the simulation results. This comparing can confirm the uncertainties that arise during the simulation calculation process.

4. ACKNOWLEDGEMENT

This study was supported by a grant of the Korea Institute of Radiological and Medical Sciences (KIRAMS), funded by Ministry of Science and ICT (MSIT), Republic of Korea. (No. 50422-2023).

5. REFERENCES

1. Kim, S., Kim, G. S., Heo, J., & Ahn, Y. (2021). Evaluating Activation for 50 MeV Cyclotron Irradiation Service using Monte Carlo Method and Inventory Code. Journal of the Korean Society of Radiology, 15(4), 415-427.

2. McGinley, P. H., & White Jr, T. A. (1983). Air activation produced by high- energy medical accelerators. Medical physics, 10(6), 796-800.

3. Farhood, B., Ghorbani, M., Goushbolagh, N. A., Najafi, M., & Geraily, G. (2020). Different methods of measuring neutron dose/fluence generated during radiation therapy with megavoltage beams. Health physics, 118(1), 65-74.

4. Agosteo, S., Birattari, C., Caravaggio, M., Silari, M., & Tosi, G. (1998). Secondary neutron and photon dose in proton therapy. Radiotherapy and oncology, 48(3), 293-305.

5. Xu, J. K., Su, Y. W., Li, W. Y., Yan, W. W., Chen, X. M., Mao, W., & Pang, C. G. (2016). Evaluation of neutron radiation field in carbon ion therapy. Chinese Physics C, 40(1), 018201.

6. Poje, M., Ivković, A., Jurković, S., Žauhar, G., Vuković, B., Radolić, V., ... & Faj, D. (2014). The neutron dose equivalent around high energy medical electron linear

accelerators. Nuclear Technology and Radiation Protection, 29(3), 207-212.

7. Banaee, N., Goodarzi, K., & Nedaie, H. A. (2021). Neutron contamination in radiotherapy processes: a review study. Journal of Radiation Research, 62(6), 947-954.

8. Anderson, C. A., Mckinney, G. W., & Tutt, J. R. (2017). Neutron & Gamma Correlations using CGM in MCNP 6.2. 0. Transactions of the American Nuclear Society, 116, 939-942.

9. Zheng, Y., Newhauser, W., Klein, E., & Low, D. (2009). Monte Carlo simulation of the neutron spectral fluence and dose equivalent for use in shielding a proton therapy vault. Physics in Medicine & Biology, 54(22), 6943.

10. McConn, R. J., Gesh, C. J., Pagh, R. T., Rucker, R. A., & Williams III, R. (2011). Compendium of material composition data for radiation transport modeling (No. PNNL-15870 Rev. 1). Pacific Northwest National Lab.(PNNL), Richland, WA (United States).

11. Jeffries, B. D., Algiere, C., Gallagher, J. A., Nichols, T. H., So, J. R., Littlefield Jr, C. W., ... & Brockman, J. D. (2019). Characterization of the neutron flux during production of ^{18}F at a medical cyclotron and evaluation of the incidental neutron spectrum for neutron damage studies. Applied Radiation and Isotopes, 154, 108892.

12. Petoussi-Henss, N., Bolch, W. E., Eckerman, K. F., Endo, A., Hertel, N., Hunt, J., ... & Zankl, M. (2010). Conversion coefficients for radiological protection quantities for external radiation exposures. Annals of the ICRP, 40(2-5), 130-131.

13. Lee, J.-A. (2022). Evaluation of Cancer Incidence Rate using Exposure Dose to Surrounding Normal Organs during Radiation Therapy for Prostate Cancer. Journal of the Korean Society of Radiology, 16(3), 351–356. https://doi.org/10.7742/JKSR.2022.16.3.351

14. Ferrari, A., Pelliccioni, M., & Pillon, M. (1997). Fluence to effective dose conversion coefficients for neutrons up to 10 TeV. Radiation Protection Dosimetry, 71(3), 165-173.